Reprinted from Preprint Volume, 14th Conference on Severe Local Storms, October 29 - November 1, 1985, Indianapolis, Ind. Published by the American Meteorological Society, Boston, Mass.

11.3

THE ROTOR MICROBURST: A NEW EXPLANATION FOR BURST SWATH DAMAGE

Brian R. Waranauskas

The University of Chicago
Chicago, Illinois

1. INTRODUCTION

Findings from the NIMROD and JAWS field projects and aerial surveys of severe storm damage areas have resulted in a highly detailed categorization of the downburst/microburst phenomenon (Fujita, 1985). As analysis is performed on smaller spatial scales, more elements are found to enhance the understanding of downburst structure and behavior. Two such elements, the burst swath and the rotor microburst, are investigated in this paper and a possible relationship between them is proposed.

2. BURST SWATHS

The smallest member of the downburst family is the burst swath, defined as being a tract of misoscale wind damage occurring within a downburst or microburst (Fujita and Wakimoto, 1981). Since these swaths are sometimes long and narrow, the damage pattern is often mistaken as that of a tornado. However, the vector pattern within the swath is uni-directional and divergent (Fig. 1), showing few rotational characteristics as found in tornado damage. Typically, the horizontal dimension of a burst swath is 100-800 meters.

Until recently, burst swaths had only been observed, with its generating mechanism never being explored in great depth. Even now the overall picture is not complete, but new research indicates that a stage in the life cycle of a microburst may offer a possible explanation as to the cause of burst swaths.

Fig. 1 Aerial photo of flattened trees in two burst swaths which occurred on 16 July 1980 near Battle Creek, MI. Photo by Roger Wakimoto.

3. ROTOR MICROBURSTS

Drawing from the analysis of JAWS wind events and the Andrews AFB microburst (Fujita, 1983), University of Chicago researchers have been able to classify different stages or phases in a microburst's evolution. Presently, there are three documented phases: 1.) the mid-air stage, 2.) the contact or touchdown stage, and 3.) the surface or spreading stage. It is in this last stage that most field observations have been made, both visually and by Doppler radar.

In the course of research, a discrepancy developed between the measured microburst wind at the ground (i.e. the wind in stage three) and the downdraft speed during the mid-air stage. In some cases the surface wind as measured by anemometers exceeded 25 m/s (56 mph), while the vertical velocity of the downflow was only 5-10 m/s (11-22 mph). Dynamically, the downflow itself could not produce such strong outflows; another mechanism must be active during the surface phase to account for the low-level wind maxima.

The first clues to a possible solution for explaining this unknown mechanism were derived from a series of photographs taken by the author while at the JAWS Project. A picture from this series is displayed in Figure 2. As

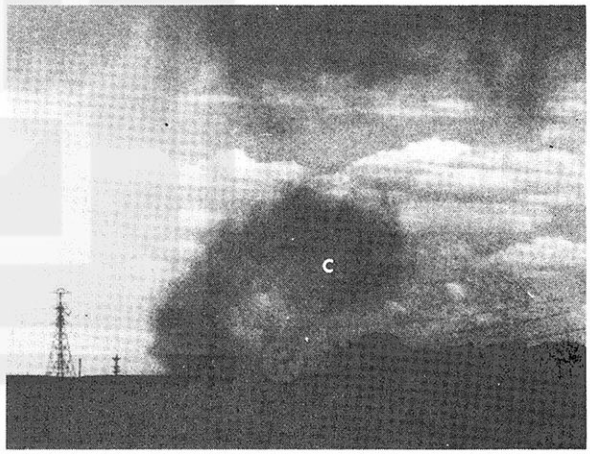

Fig. 2 Ground photo illustrating the curling structure along the leading edge of a microburst's outflow. The curl is made visible by dust blown upward from the surface. Photo by the author, taken near Brighton, Colorado on 15 July 1982.

seen in the photo, there is a very noticeable vertical curl of dust along the leading edge of a microburst's outflow, as well as indicating the presence of a horizontal axis of rotation with its center located well above ground level (denoted by the 'C' on the photo). Because of the strong rotary motion about this axis, such an outflow structure was named a "rotor microburst" (Fujita, 1985), or more precisely, the rotor sub-stage of a microburst outflow.

From this visual observation it was proposed that microburst and ambient air circulating in the vertical plane of the rotor could be sufficiently accelerated near ground level to produce a local area of extreme wind. Hence, a weak or moderate downdraft could produce strong surface winds if a rotor circulation develops in the outflow regime.

4. DOPPLER SYNTHESIS AND MULTI-SCALE ANALYSIS

To enhance this inital hypothesis, multiple Doppler synthesis and miso- and mesoscale analysis of a significant JAWS microburst (30 June 1982, 1831 MDT at PAM Station 23) was performed to document the horizontal and vertical structure of a rotor microburst. Figure 3 depicts the PPI presentation of this case, showing the microburst advecting away from the southeast edge of the parent storm cell. At the analysis time, the rotor axis is passing over PAM 23, giving a peak windspeed of 29.1 m/s (65 mph).

The RHI cross-section for the same time is presented in Figure 4. Note the reversal in direction of the Doppler velocities at 1.0-1.5 km AGL. The upper-level flow toward the radar (negative velocities) is in response to a misocyclone aloft which was located northeast of the PAM site at this time (Kessinger et al. 1984). The low-level wind maximum at 9 km range is the microburst which struck the PAM station.

The structure of the rotor is best seen in Figure 5, where the the axis of rotation is clearly defined by the absolute motion vectors. One observes that the axial center is not at ground level, but instead at 800 m AGL, consistent with the photo in Figure 2. As the area of highest surface wind is directly beneath the circulation center, where confluence between the ground and the axis is greatest. Also seen is a precipitation roll, defined by the 30 and 35 dBZ contours at the 10.5 km range. This roll is composed of water droplets from the echo region being blown forward by the rotor's winds, similar to that found in gust front studies (Wakimoto, 1981). In a dry microburst (no precipitation reaching the ground during the high winds) this roll may be composed of dust or smoke drawn up from the ground.

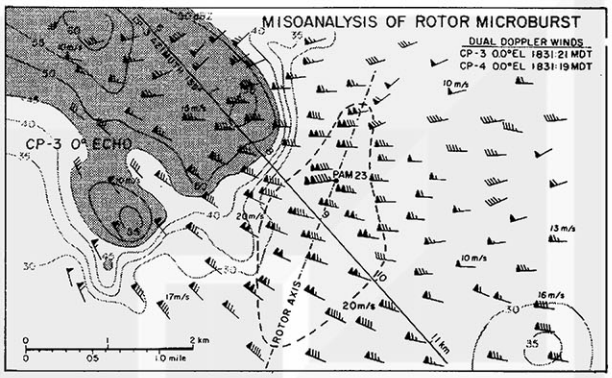

Fig. 3 Misoscale dual-Doppler analysis of the rotor microburst of 30 June 1982 during the JAWS Project. Reflectivities are represented by the gray isolines. Note that the maximum surface wind at PAM 23 occurred as the rotor axis passed over the station.

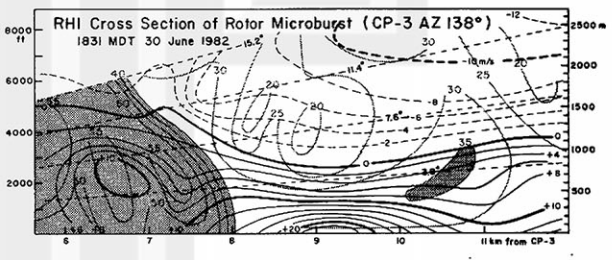

Fig. 4 RHI view of the 30 June rotor stage. Doppler velocities are in m/s with dashed contours indicating flow toward the radar (left) and solid contours sinifying flow away from the radar (right). Gray areas are storm reflectivities.

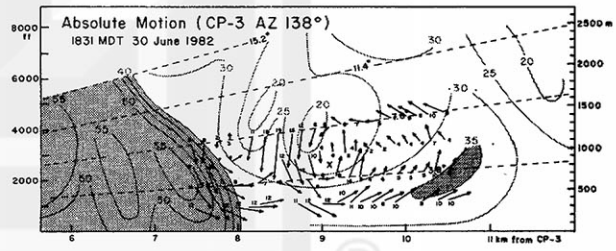

Fig. 5 Absolute motion of the rotor stage. Vectors are in m/s. The X denotes the center of the axis of rotation.

The wind and pressure traces from PAM 23 for the 30 June case are displayed in Figure 6. the wind profile shows the characteristic short-lived spike of high windspeed as the microburst hits the observing station, highlighted by a 17.7 m/s (40 mph) increase in the maximum velocity between 1830 and 1831 MDT. Of greater interest is the pressure trace. The curve actually shows two atmospheric effects happening simultaneously. The overall dip, as defined by the ends of the curve and the dashed line, is the local response to the passing of the misocyclone aloft. Superimposed upon this pattern is the pressure fluctuation caused by the microburst. The strong rises and drops of the microburst profile result from the total pressure of the outflow being converted into velocity pressure. At microburst center the total pressure is a maximum but decreases proportionally to increases in outflow velocity. Thus, one would expect to find the peak windspeed at the point of lowest pressure, which is the case here. In the presence of a well-defined rotor, the lower ambient pressure at the rotor core acts to accelerate the surface winds thereby making the axial center and the microburst coincident on spatial and temporal scales, as previously noted.

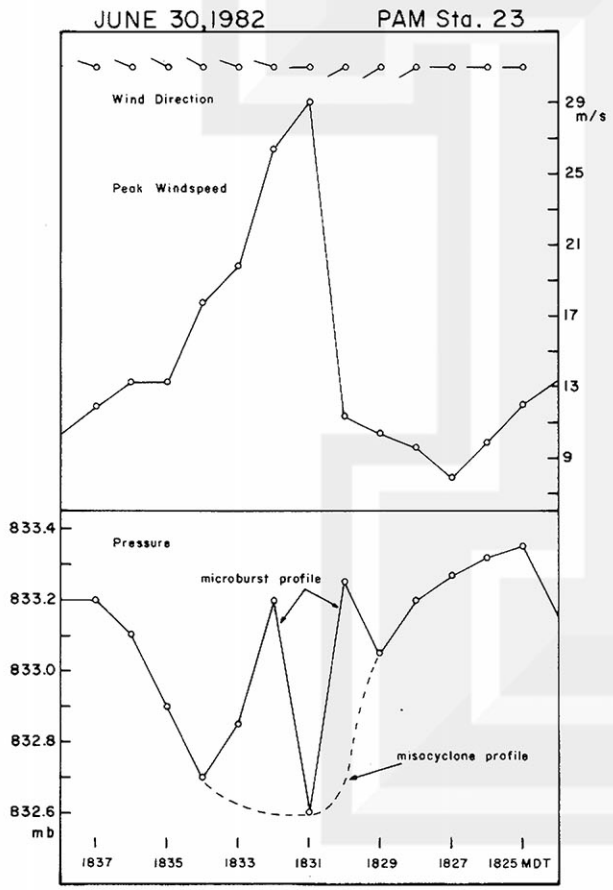

Fig. 6 PAM station time section of the 30 June microburst. Maximum windspeed correlates well with lowest pressure. Pressure curve shows simultaneous passage of the microburst and a misocyclone.

5. A ROTOR MICROBURST/BURST SWATH MODEL

With the rotor sub-stage now established visually and analytically in the atmosphere, a final element, that of laboratory simulations, can be added to devise a plausible model. Recent lab simulations at the University of Chicago highlight the importance of a microburst's pre-rotor evolution in explaining the role of the rotor in burst swath occurrence.

The photograph in Figure 7 is a laboratory microburst in the mid-air stage. The key point of this picture is the appearance of a horizontally oriented vortex ring surrounding the downdraft. This ring is the first step in rotor development. Conceptually, as the downdraft continues to propagate to the surface, the vortex ring is maintained and begins to stretch outward in the diverging flow. In time the vortex undergoes more expansion until it reaches some

Fig. 7 Photo of a lab simulated microburst in the mid-air stage. The horizontal vortex ring is the parabolic feature at the leading edge of the downdraft column. Photo by T. Fujita.

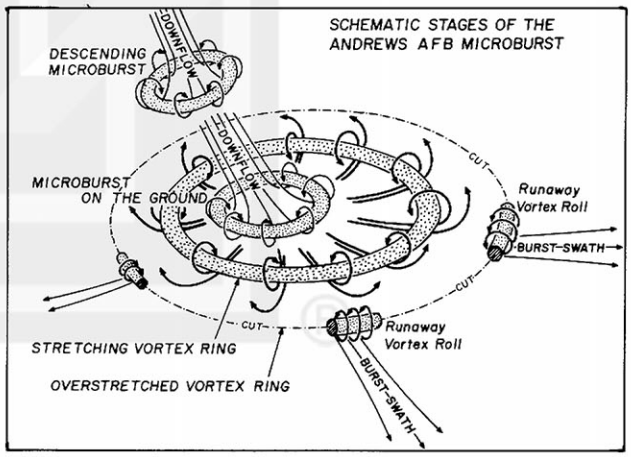

Fig. 8 Schematic diagram of the proposed model as derived from analysis of the Andrews AFB microburst. From Fujita (1983).

stretching limit at which it begins to break-up. the strongest sections of the ring continue to propagate in quasi-radial paths. These individual vortex segments stretch further and take on the characteristic rotor shape. Translation of the segments near the surface can produce burst swaths as the wind velocity about the rotor axis reaches 25-50 m/s (56-112 mph), causing light to moderate damage (F0-F2) to trees, buildings, and other ground structures. A schematic illustration of this model is presented in Figure 8.

6. CONCLUSION

Thus, a preliminary working model of the rotor microburst/burst swath relationship is proposed. The roles of the parent vortex ring and the pressure/velocity exchange are found to be very important and additional research on these elements should provide insight for modification of the initial model. Also, future work must incorporate the theoretical findings of analogous situations in fluid dynamics, thereby completing the overall understanding of all parts of the rotor microburst/burst swath event.

ACKNOWLEDGEMENTS

The author would like to thank Dr. T. Theodore Fujita for his guidance and for first formulating the rotor concept. Special thanks is also given to Mr. James Partacz who went beyond the call of duty in preparing the photographic work used in this paper. This research is sponsored by NASA grant NGR 14-001-008, NOAA/NESDIS grant NA85AADRA064 and NSF grant ATM 8109828.

REFERENCES

Fujita, T.T., 1983: The Andrews AFB microburst. SMRP Research Paper 205, Univ. of Chicago, 38 pp.

Fujita, T.T., 1985: The Downburst. Satellite and Mesomet. Res. Proj., Chicago, 122 pp.

Fujita, T.T., and R.M. Wakimoto, 1981: Five scales of airflow associated with a series of downbursts on 16 July 1980. Mon. Wea. Rev., 109, pp 1438-1456

Kessinger, C.J., M.L. Weisman, J. Klemp, and J. Wilson, 1984: The evolution of mesoscale circulations in a downburst-producing storm and comparison to numerical results. Preprints 22nd Conf. on Radar Met., Geneva, Amer. Meteor. Soc.

Wakimoto, R.M., 1981: Investigations of thunderstorm gust fronts using Project NIMROD data. Ph.D. thesis, Dept. of Geophys. Sci., Univ. of Chicago, 129 pp.